Clustering of asymmetric dumbbell-shaped silica/polystyrene nanoparticles by solvent-induced self-assembly

Weiya Li, Serge Ravaine, Etienne Duguet

Clustering of asymmetric dumbbell-shaped silica/polystyrene nanoparticles by solvent-induced self-assembly

Weiya Li,[a,b] Serge Ravaine[b] and Etienne Duguet [a]*

a. Univ. Bordeaux, CNRS, ICMCB, UMR 5026, F-33600, Pessac, France. Email : etienne.duguet@icmcb.cnrs.fr

b. Univ. Bordeaux, CNRS, CRPP, UMR 5031, F-33600, Pessac, France

Abstract

We report a quite simple strategy to assemble silica/polystyrene dumbbell-shaped nanoparticles into clusters with an aggregation number from two to more than 30. The polystyrene lobe serves as a patch that is made sticky and ready to merge with similar ones when the dumbbells are dispersed in an ethanol/DMF mixture. Thanks to transmission electron microscopy experiments, we describe qualitatively and quantitatively the influence of several experimental parameters such as the solvent quality, i.e. DMF fraction, and the patch-to-particle size ratio. We show that the DMF fraction range (30-50 vol. %) for the sticky regime can be extended if the incubation process is completed by a centrifugation step. We also demonstrate an unexpected evolution in the average aggregation number with the patch-to-particle size ratio that may be explained by the molar mass distribution within the polystyrene core of the clusters. Lastly, we show that this assembly route may be extended to gold-coated clusters.

Keywords: silica/polystyrene nanoparticles; solvent-induced assembly; patch-to-particle size ratio; gold-decorated silica clusters

Introduction

In recent decades the efforts of chemists combined with ever more efficient characterisation techniques have made it possible to develop more and more complex solid colloids. In particular the anisotropy of shape and/or chemical composition is particularly sought after because it makes it possible to program assembly capabilities into structures of larger dimensions. Thus Janus particles [1–3] and more recently patchy particles [4–6] have attracted significant attention as potential building blocks on both simulation and experimental aspects.

Among Janus particles, asymmetric dumbbells and snowman-like colloids are of special interest if (i) one of the two lobes is hard and potentially repulsive and

the other is attractive, and (ii) they self-assemble into clusters with small aggregation numbers *N*, often called “colloidal molecules”. Some previous studies showed that this strategy may be used with colloids of several tens of nanometres [7–9], a few hundred nanometres [10], a couple of micrometres [11–17] or a couple hundred micrometres [18]. Nevertheless, most of these clusters were obtained thanks to solvophobic interactions [8,9,12,13], electrostatic attraction [7,11], roughness-controlled depletion forces [14], lipid-induced capillary bridging [15], or surfactant mediation [17], which are weak and can be made reversible.

To get more robust clusters, it may be envisioned that the attractive lobe should be sticky and possibly capable of merging with similar ones. Kraft *et al.* reported an original pathway where the sticky lobe is a monomer protrusion ready to coalesce before solidification by polymerisation [10]. These protrusions are spontaneously formed when crosslinked polystyrene (PS) particles are made hydrophilic by surface modification with vinyl acetate, dispersed in water, swollen with styrene and heated to 80°C. The final clusters with *N* from 2 to 9 are more readily described as spherical hydrophilic particles with a defined number of hydrophobic PS patches [10]. When the swelling ratio is increased, the relative volume of the protrusion is higher and the final patchy colloids are less symmetrical but mimicking surprisingly the space-filling models of H_2O or NH_3 molecules [19]. Bon and coll. prepared micron-sized asymmetric dumbbells made of a PS sphere and a poly(n-butylacrylate) (PBA) lobe and showed their ability to form well-defined clusters when dispersed in aqueous media [16]. The assembly process is induced by the desorption of the poly(vinylpyrrolidone) stabiliser from the particles and the merging of the soft PBA lobes upon contact through collision. More recently, Xu and co-workers exploited the drying of Pickering-like water droplets made from 200 µm hydrophilic poly(ethylene glycol) diacrylate sphere with 160 µm ethoxylated trimethylolpropane tri-acrylate lobe prepared by a microfluidic technology [18]. They obtained quite regular submillimetre-sized clusters with *N* up to eight.

We report here another strategy using silica/PS dumbbells (in the size range of 100-200 nm) whose PS lobe is plasticised, *i.e.* made sticky, and ready to coalescence when the dispersion medium is a suitable mixture of a good and a bad solvent. This leads to multipod-like clusters made of one PS core and some silica satellites. Moreover, this is the reverse morphology of highly symmetrical multipods that we have already reported considering that PS and silica switch their roles [20].

For this study, we could have used the silica/PS monopods that we know how to prepare according to the seeded growth emulsion polymerisation process [21]. Nevertheless, the PS lobe, *i.e.* the patch, would have been much larger than the silica lobe and not easily down sizable. So we prepared them according to a protocol previously reported by Guignard and Lattuada [22] (Fig. 1) and took advantage of this synthesis pathway to vary the size of the PS lobe, *i.e.* the patch-to-particle size ratio. We triggered their assembly by making their PS lobe sticky through incubating in mixtures of ethanol and dimethylformamide (DMF) which are bad and good solvents for PS, respectively. We especially studied several experimental parameters such as the solvent quality, effect of an additional centrifugation stage after incubation, dumbbell concentration, incubation time, and patch-to-particle size ratio. We also extended this facile method to the fabrication of gold-coated silica clusters. The dumbbell and cluster morphology was essentially estimated qualitatively and quantitatively from transmission electron microscopy (TEM) images.

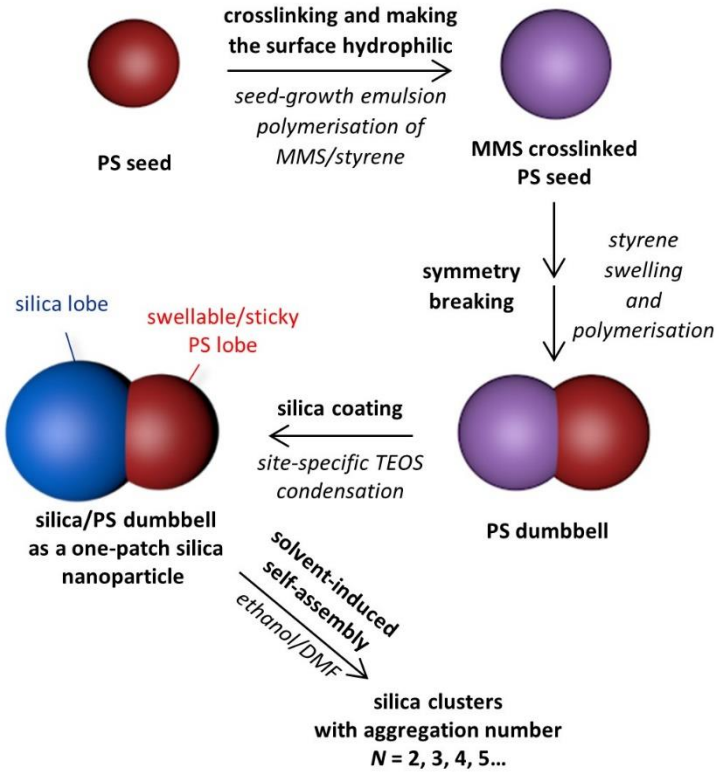

Fig. 1 Scheme showing the synthesis pathway to get silica/PS dumbbells and their subsequent solvent-induced assembly.

Experimental

Synthetic procedures

Materials. Styrene (99.5%, with c.a. 50 ppm 4-tert-butylcatechol as stabiliser), sodium dodecyl sulphate (SDS, 99%), 4-vinylbenzenesulfonate (VBS, ≥90%), tetraethoxysilane (TEOS, ≥99%), dimethylformamide (DMF, ≥99%), sodium persulfate (NaPS, ≥99%), (3-aminopropyl)triethoxysilane (APTES, 99%), hydroxylamine hydrochloride ($NH_2OH{\cdot}HCl$, 98%), gold chloride hydrate ($HAuCl_4$, 99.999%), potassium carbonate (K_2CO_3) and tetrakis(hydroxymethyl)phosphonium chloride solution (THPC, 80% in water), sucrose (grade puriss.) and sodium hydroxide (≥98.5%, microprills) were purchased from Sigma-Aldrich. Methacryloxymethyltrimethoxysilane (MMS, 95%) was provided by ABCR, Germany. Ammonium hydroxide (NH_4OH, 28-30% in water) was purchased from JT. Baker and ethanol (99%) was provided by Atlantic Labo. 2,2′-Azobis(2-methylpropionitrile) (AIBN, 98%) was received from Acros Organics. Deionised water with a resistivity of 18.2 MΩ.cm at 25°C was obtained from a Milli-Q system (Millipore). All chemicals were used without further purification.

Synthesis of dumbbell-shaped polystyrene/silica nanoparticles. They were prepared according to a previously reported multistep protocol [22]. First, PS latex particles were obtained by conventional emulsion polymerisation (75°C, 400 rpm, 12 h) using water (83.75 mL), SDS (1 g), styrene (20 g) and $Na_2S_2O_8$ (0.1 g) in a nitrogen-degassed 250 mL three-neck flask. The monomer-to-polymer conversion determined by the dry extract method was 97%. Second, the latex particle surface was simultaneously crosslinked and made hydrophilic through encapsulation in a shell of *in situ* synthesised poly(styrene-*co*-MMS). Briefly, the as-obtained latex dispersion (50 mL, 90 g/L) was mixed with water (84 mL) and a mixture of styrene, MMS (20 wt.% to total monomer) and AIBN, where the total volume of monomer equals to the volume of PS particles and the amount of AIBN is 3% wt./vol. to total monomer. After nitrogen-degassing for 40 min under 300 rpm magnetic stirring, the polymerisation was initiated by increasing the temperature to 75°C, and maintained for 12 h to reach a monomer-to-polymer conversion of 94%. Third, the as-obtained core-shell nanoparticles (NPs) were made dissymmetrical, *i.e.* dumbbell-shaped, by controlled phase separation in the course of a third polymerisation step after styrene-swelling. Briefly, a mixture made of the latex dispersion (20 mL, 60 g/L), water (40 mL) and VBS (0.8% wt./vol. to total monomer) was nitrogen-degassed for 30 min under 400 rpm magnetic stirring. Then, a given volume of styrene with AIBN (3% wt./vol. to monomer) was added in order to obtain the targeted swelling ratio *S*, *i.e.* styrene-to-particle volume ratio. Three hours later, the temperature was increased to 75°C and maintained for 12 h. The monomer-to-polymer conversion was 49%, 70%, 93%, 84% and 98% when *S* was equal to 0.5, 1, 2, 3 and 5, respectively. Fourth, a silica shell was regioselectively grown onto the

hydrophilic moiety of the dumbbells following a protocol adapted from the conventional Stöber's process.[23] Typically, for a 20-nm-thick silica coating, the dumbbell dispersion (10 mL) and ammonia (5.1 mL) were added to 67 mL ethanol and stirred at 400 rpm. Then, a solution of TEOS (3.6 mL diluted with 3.6 mL ethanol) was injected at a flow rate of 0.5 mL/h and allowed to react overnight. The particles were washed in ethanol by 3 centrifugation/redispersion cycles (12,000 g; 10 min; 85 mL). The final concentration was estimated to be 1.12×10^{16} part/L.

Gold deposition on the silica part of the dumbbells. The seeded growth protocol was inspired by previous reports concerning other nanosized substrates [24,25]. First, the silica surface was aminated by reaction of APTES used at the concentration of 50 molecules per nm^2 of silica surface at room temperature (RT) for 15 h in ethanol. The particles were extracted by centrifugation (12,000 g) and redispersed in 1 mL ethanol in a 15 mL tube. Then, 5 mL THPC-stabilized gold seeds dispersion in water, prepared according to the Duff's protocol [26] from $HAuCl_4$, THPC and NaOH and aged for at least 3 days at 4°C, were added. Then the tube was put on a roller-mixer at 60 rpm for 6 h. The Janus-like dumbbell particles were separated from the excess THPC-stabilized gold seeds through 3 centrifugation/redispersion cycles (12,000 g; 10 min; 6 mL) and finally redispersed in 1 mL ethanol. Lastly, the regrowth of the adsorbed gold seeds was carried out using a gold plating solution. Two stock solutions were prepared: solution #1 by dissolving $NH_2OH{\cdot}HCl$ (130 mg) in water (1 L) and solution #2 by dissolving K_2CO_3 (130 mg) in an aqueous $HAuCl_4$ solution (1 L, 0.375 mM). The latter solution was aged at 4°C for 1 day before use. The seeds were regrown by mixing the gold-decorated dumbbell dispersion (0.1 mL), water (10 mL), solution #2 (10 mL) and adding dropwise solution #1 (5 mL) at a rate of 10 mL/h under vigorous stirring. The as-modified particles were collected by centrifugation (12,000 g) and redispersed in 0.1 mL ethanol. This protocol was iteratively repeated to obtain the targeted thickness of the gold coating.

Self-assembly of the dumbbells into clusters. The self-assembly experiments were routinely performed in 1.5 mL Eppendorf® tubes and the sum of the DMF and ethanol volumes was systematically equal to 1 mL. For instance, we mixed the previous ethanol dispersion of silica/PS dumbbells (47 µL), DMF (300 µL) and ethanol (653 µL) together by vortexing for 30 s. The Eppendorf® tubes were put on a roller-mixer at 60 rpm for 20 min or 20 h at RT to induce the assembly process. For TEM analysis, a drop was directly collected from the dispersion and allowed to evaporate on a TEM grid. Alternatively, the dispersion was centrifuged at 12,000 g for 10 min and the pellet redispersed in ethanol after removing the supernatant prior to TEM grid preparation.

Density gradient centrifugation. A gradient maker (BioComp Gradient Master™ 108) was used to prepare a 5-20 wt./vol.% linear gradient of sucrose in water at 4°C. Five hundred µL of the cluster suspension were carefully loaded on top of 12 mL of gradient before centrifuging with a TH-641 swinging-bucket rotor (Thermo Fisher Scientific) for 20 min at 8,000 g and 4°C. A BioComp Piston Gradient Fractionator™ was used to pull out individual bands from the sample. The fractions were purified by several centrifugation-redispersion cycles (8,000 g; 4 min) in water.

Characterisation techniques

Transmission electron microscopy. TEM images were obtained on Hitachi H600 or JEOL 1400 microscopes operating at 75 kV or 120 kV, respectively. Typically, the particles diluted with ethanol were dropped directly on carbon-coated copper films (300 mesh) and ethanol was allowed to evaporate at RT. Statistics from image analysis were performed using at least 300 nano-objects for the seeds, 500 for the dumbbells and 250 for their assemblies. The size polydispersity index (PDI) was calculated according to the following equation:

$$PDI = \frac{\overline{D_w}}{\overline{D_n}} = \frac{\sum n_i \sum n_i d_i^4}{\sum n_i d_i \sum n_i d_i^3}$$

Results and discussion

Synthesis of the asymmetric dumbbell-shaped building blocks

Silica/PS dumbbell-shaped nanoparticles (NPs) were obtained after a multistep pathway reported by Guignard and Lattuada (Fig. 1) [22]. This protocol includes two successive seeded-growth emulsion polymerisation stages from conventional PS latex particles. The first one creates a thin hydrophilic and crosslinked shell by copolymerizing randomly styrene and methacryloxymethyltrimethoxysilane (MMS). The second one takes advantage of the elastic stress generated by the crosslinked shell when the particle is swollen again with styrene. This causes a phase separation forcing the new generation of PS macromolecules to create a lateral protrusion. This phenomenon was exploited since the ‘90s to prepare asymmetrical latex particles [27] and was recently revisited and extended to multilobe morphologies [28]. The last step consists in creating a silica half-shell covering specifically the hydrophilic hemisphere of the dumbbells.

The precursor seeds, *i.e.* the spherical PS latex particles, were prepared by conventional emulsion polymerisation of styrene initiated by the thermal

decomposition of $Na_2S_2O_8$ in water in the presence of sodium dodecylsulfate. Their number-average diameter is 59 nm with a polydispersity index PDI = 1.08 (See Supplementary material, Fig. S1).

After the growth of the crosslinked shell by seeded-growth emulsion copolymerisation of styrene and MMS, the average diameter of the particles increased from 59 to 71 nm with PDI = 1.10 (See Supplementary material, Fig. S2a). The presence of MMS units along the PS chains was checked by infrared spectroscopy showing the appearance of specific bands at 1100 cm^{-1} and 1720 cm^{-1} assigned to Si-O-C/Si-O-Si and C=O vibrations, respectively (See Supplementary material, Fig. S2b). Actually, the absence of C=C band in the 1637 cm^{-1} range and the presence of the Si-O-Si band indicate that the MMS monomer was essentially attached to the macromolecules through the copolymerisation scheme and that a fraction of the methoxy groups reacted together and therefore served as crosslinking points. The hydrophilic character of these shell-crosslinked PS seeds was evidenced qualitatively by showing that henceforth the seeds are easily transferred from hexane to water (See Supplementary material, Fig. S2c).

To create the protrusion changing the particle morphology from sphere to dumbbell, pure styrene was used to swell the MMS-crosslinked PS particles. The minimum time to reach the swelling equilibrium was shown to be 3 h (against 1 h as reported by Guignard and Lattuada [22]), because polymerisation experiments initiated even after 2 h showed the presence of small latex particles, resulting from a homogeneous nucleation process (See Supplementary material, Fig. S3). The polymerisation was performed in surfactant-free conditions facilitated by the presence of a very low amount of 4-vinylbenzene sulfonate comonomer introduced before styrene-swelling. Experiments were first performed with a swelling ratio, *i.e.* styrene-to-particle volume ratio, $S = 2$. The heating procedure afterwards caused phase separation driven by elastic stress [29–31], and the wetting angle between the protrusion and seed was determined by the hydrophilicity of the seed surface [10]. Therefore, the polymerised protrusion was observed in TEM experiments (Fig. 2). The dumbbell yield is 97% from image analysis. The presence of smaller dumbbells is due to the quite large size distribution of the initial PS seeds. Whatever the seed size, the diameter of the protrusion (typically 68 nm) is close to that of the seed whose average diameter increased slightly from 71 to 75 nm. We varied the swelling ratio ranging from $0.5 < S < 5$, and we observed that the higher the S value, the larger the PS protrusion relative to the MMS-crosslinked

PS seed, as previously reported [32]. In this way, we obtained snowman-like morphologies for $S < 2$ and "reverse" snowman-like ones for $S > 2$ where the PS lobe represents henceforth the body of the snowman.

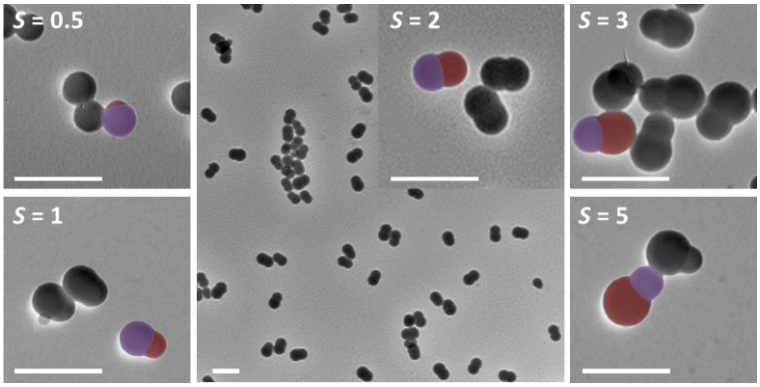

Fig. 2 Representative TEM images of dumbbell-shaped PS NPs obtained for different values of the swelling ratio *S* (scale bars: 200 nm). For the sake of clarity, the MMS-crosslinked PS seed and the PS protrusion have been falsely coloured in violet and red, respectively, for one particle on each enlarged TEM image.

Lastly, the polycondensation of TEOS specifically on the hydrophilic part of the dumbbells was carried out using conventional Stöber conditions, *i.e.* in hydro-alcoholic medium using ammonia as a catalyst [23]. TEM images show that only the hydrophilic nodule is enlarged (Fig. 3). The silica coating thickness was found to be $E \approx 20$ or 35 nm (for $S = 2$) according to the used amount of TEOS. This dissymmetrical coating was confirmed by a calcination stage at 600°C removing the pure PS component and leading to silica nanobowls with a regular thickness (See Supplementary material, Fig. S4) as previously reported [22].

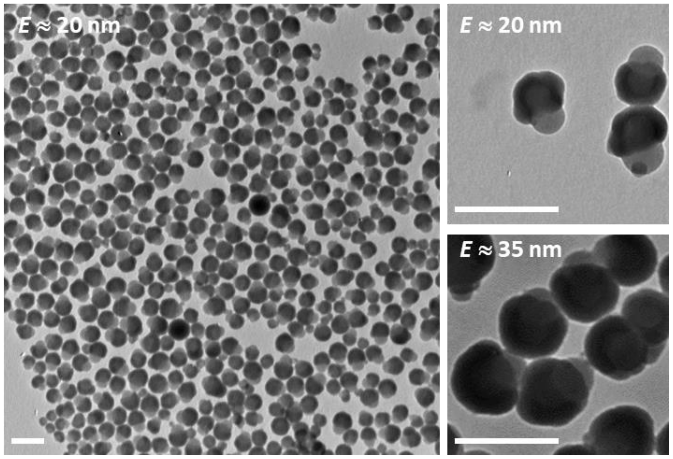

Fig. 3 Representative TEM images of the asymmetric dumbbell-shaped silica/PS NPs ($S = 2$) with different values of the silica coating thickness *E* (scale bars: 200 nm).

According to the same strategy, several batches of asymmetric dumbbells were prepared with different geometrical features (Table 1), in particular with a patch-to-particle diameter ratio varying from 0.32 to 1.00.

Table 1 Geometrical features of the prepared asymmetric dumbbell-shaped silica/PS NPs.

Batch	Swelling ratio *S*	Silica coating thickness *E* (nm)*	Silica lobe diameter *D* (nm)*	PS lobe base diameter *d* (nm)*	Patch-to-particle size ratio d/D
#1	0.5	20	110	35	0.32
#2	1	20	110	50	0.45
#3	2	20	110	68	0.62
#4	2	35	140	68	0.49
#5	3	20	110	90	0.82
#6	5	20	110	110	1.00

* every dimension is given as an average round value and shall be considered with an accuracy of ± 3 nm

Solvent-induced assembly: effect of the solvent quality and centrifugation force

This series of experiments was carried out with the silica/PS dumbbells of Batch #3, initially dispersed in ethanol. The procedure consisted of adding a mixture of DMF/ethanol at RT and letting the particles age for 20 h under gentle stirring. The experiments were performed in similar conditions in Eppendorf® tubes with a total liquid amount of 1 mL and a concentration of 5.3×10^{14} part/L. Unlike ethanol, DMF is a good and solvent for PS. It means that DMF molecules are prone to develop interactions with the PS macromolecules to the extent that phenomena of plasticisation, swelling and dissolution occur successively for larger and larger amounts of DMF. The self-assembly of the dumbbells by their PS lobe can be described as a three-stage process: the contact promoted by hydrophobic interactions, the merging of the lobes facilitated by DMF plasticization/swelling and the physical entanglement of the PS chains originating from different lobes upon liquid removal.

Fig. 4 summarises the self-assembly results when the DMF fraction in the mixture was progressively increased every 10 vol. %. We performed statistical analyses of the TEM images over more than 250 species in order to assign an aggregation number to each of them: $N = 1$ for unassembled dumbbell-shaped NPs, $N = 2$ for clusters made of two NPs, *i.e.* bipods, $N = 3$ for tripods, etc. In

the graph (Fig. 4f), the prevalence of a cluster type is quantified through the fraction of initial silica/PS dumbbells used to obtain it and represented by blue disks whose surface is proportional to this fraction. Three main situations as a function of the DMF amount can be observed:

i) in the 0-20 vol. % range, the amount of DMF was too low to swell the PS lobes efficiently and make them sticky. Therefore, this is a “non-solvent regime”, and the silica/PS dumbbells remain intact and unassembled (*N* = 1);

ii) in the 30-50 vol. % range, the DMF fraction made the solvent quality better and better and clusters with *N* values up to 4, *i.e.* tetrapods, were systematically observed (Fig. 4b). This “sticky regime” allowed at least 70% of the dumbbells to be spontaneously changed into clusters. The higher the value of *N*, the lower the prevalence of the clusters and the bipods were often the majority of the population;

iii) in the 60-90 vol. % range, the PS chains were readily solvated and quite efficiently extracted from the dumbbells leading to silica half-shells at the internal surface of which the PS segments that had been crosslinked with MMS remained covalently bonded (“solvent regime”). Therefore, the PS lobes disappeared and the as-obtained silica half-shells remained essentially unassembled.

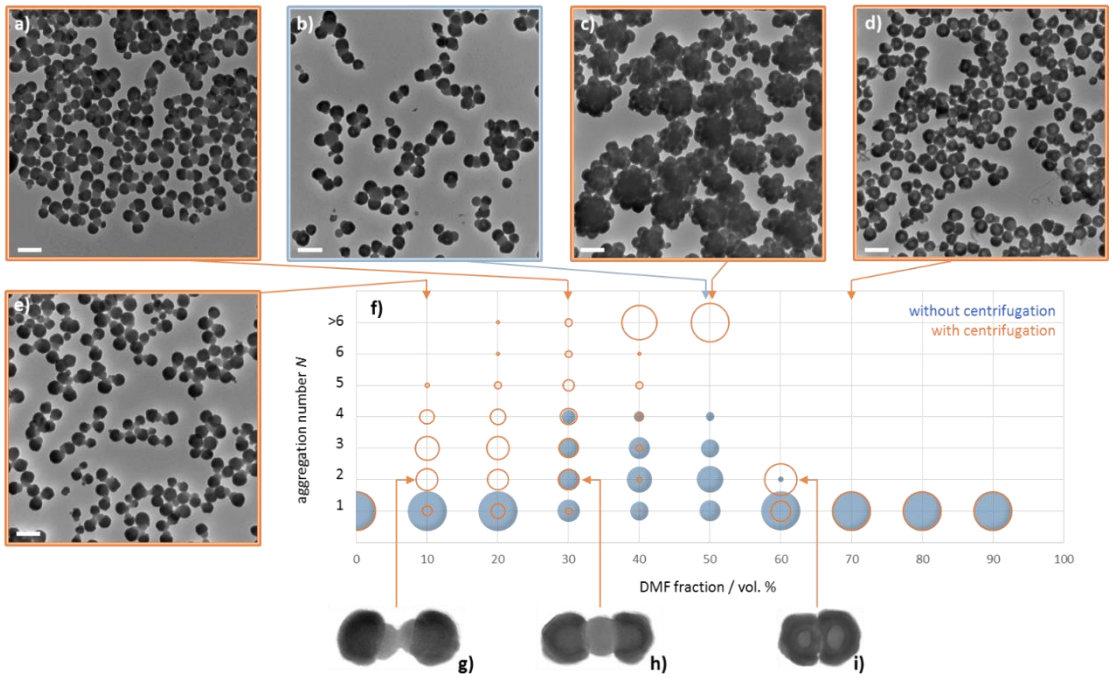

Fig. 4 a) to e) Representative TEM images of the cluster mixtures from the silica/PS dumbbell-shaped NPs as a function of the composition of the ethanol/DMF medium (scale bars: 200 nm); f) distribution of the NPs within the clusters of aggregation number *N,* as determined by statistical analysis of the TEM images (the surface of the disks and circles is proportional to the

fraction of NPs assembled within clusters of similar aggregation number); g) to i) enlarged TEM profiles of bipods (N = 2) showing the different types of bonding through the PS phase. Assembly experiments were performed with the silica/PS dumbbells of Batch #3 at a concentration of 5.3×10^{14} part/L at 20°C for 20 h with or without a final centrifugation stage (12,000 g for 10 min).

Initially, the TEM samples were prepared by dropping the cluster dispersion on the grid directly, but in the “solvent” and “sticky regimes” the image quality was often bad because of the grid pollution by the extracted PS macromolecules. In order to overcome this issue, we decided to perform a centrifugation step (12,000 g for 10 min) to remove the potentially dissolved PS macromolecules and transfer the clusters in ethanol to prepare the TEM grids. Unexpectedly, this increased quite strongly the average aggregation number $\overline{N}$ and therefore disturbed the spontaneous prevalence of the clusters (orange circles to be compared to the blue disks in Fig. 4f). It was indeed possible to observe not only new clusters with N from 5 to 8, but also large raspberry-shaped clusters with N higher than 10 up to more than 30. In the “sticky regime”, for instance for DMF fraction of 30 vol. %, the extra consumption of the dumbbells seems to be beneficial to the appearance of new clusters with N from 5 to 8 without changing the distribution within the clusters with N from 2 to 4 (Fig. 4a). Moreover, the centrifugation extends the “sticky regime” from 10 to 60 vol. % of DMF fraction (Fig. 4e). For higher DMF fractions, the centrifugation stage had no effect on the absence of self-assembly.

The large raspberry-like clusters were exclusively prevalent when the DMF fraction was 40 and especially 50 vol. % (Fig. 4c *vs* Fig. 4b). From a morphological viewpoint, the formation of the latter could result from the full entrapment of some dumbbells within the largest clusters thanks to an excessive sticky behaviour of the PS protrusion and/or the pre-adsorption of free PS macromolecules onto the silica surface lowering its surface energy. Unfortunately, it was not possible to check unambiguously for the presence of silica nodules within these largest clusters. Despite that, this assumption is supported by the fact that such raspberries were not obtained when the DMF fraction was lower, *i.e.* when the stickiness of the PS lobe and the amount of free PS macromolecules are expected to be lower.

The role of the centrifugation stage remains not fully explained: this can shift the system in a non-equilibrium state, enhance the frequency and energy of the collisions between the NPs and provide areas – especially in the pellet – where the NPs concentration tends to be maximum.

Lastly, the high-magnification TEM profiles of the bipods, *i.e.* clusters made of two silica half-shells attached face-to-face, was also very informative (Fig. 4g-i observed after the centrifugation stage). The higher the DMF fraction, the closer both half-shells. At low DMF fraction (10 vol. %; Fig. 4g), both PS lobes share only a small contact area. This means they were poorly sticky and probably the low amount of DMF allowed plasticizing/swelling just an external shell of the PS lobes. For 30 vol. % (Fig. 4h), both lobes readily fused into a single PS nodule making the bipod bonding particularly robust after DMF removal. For 60 vol. % (Fig. 4i), the contact between both silica half-shells is particularly close and the volume of the PS sticking point is minimal, *i.e.* only bipods can be obtained for evident steric reasons. Moreover, this demonstrates that a non-negligible amount of non-crosslinked PS macromolecules remain physically entangled with those that are covalently bonded, which is mandatory to ensure assembly. Indeed, since in the "solvent regime", *i.e.* for higher DMF fractions, the assembly does not occur when all the non-crosslinked macromolecules are supposed to have been extracted. This means that the macromolecules, which are covalently bonded at the bottom of the silica half-shells, are too short or not numerous enough to stick efficiently to those of another half-shell, whatever the overcrowding provided by the centrifugation stage. This conclusion was supported by a verification experiment which consisted of incubating again the silica half-shells obtained at 90 vol. % of DMF this time in "sticky conditions", *i.e.* 30 vol. % of DMF. We observed no cluster, meaning that the presence of a minimal amount of just-entangled PS chains is mandatory to achieve the self-assembly.

Because clusters were achieved not only within the targeted aggregation number range of N from 2 to 8, but also for the more robust ones, the experimental conditions for the rest of the study were set to a DMF fraction of 30 vol. % followed by a centrifugation stage. We studied also the influence of the particle concentration and the incubation time on the average aggregation number. We varied the concentration up to 5 times (See Supplementary material, Fig. S5) and observed only a slight increase of $\overline{N}$ over the concentration range of 2.65 to 3.19. This means that either the concentration range that we investigated was not large enough, or the final centrifugation stage reduced an effect that would have been more significant without it. We varied the incubation time from 5 min to 20 h (See Supplementary material, Fig. S6), but we did not observe any true plateau.

Solvent-induced assembly: effect of the patch-to-particle size ratio

Several simulation studies of somewhat similar Janus particle assemblies were reported over the last decade [33–39]. Some of these showed that the patch-to-particle size ratio is a critical parameter with regard to the packing ability of the particles [35,38]. From an experimental viewpoint, Kang and Honciuk prepared asymmetric polymeric dumbbells made of a poly(tert-butyl acrylate) lobe and a poly(3-(triethoxysilyl)propyl methacrylate) lobe of different size ratios and studied their spontaneous self-assembly in water with 10 vol.% ethanol under shear, produced by shaking or sonication [40]. In this way, they obtained different superstructures, such as capsules with different curvatures.

The silica/PS dumbbell-shaped NPs with different patch-to-particle size ratios (*cf.* Table 1) were assembled in similar conditions and representative TEM images are shown in Fig. 5.

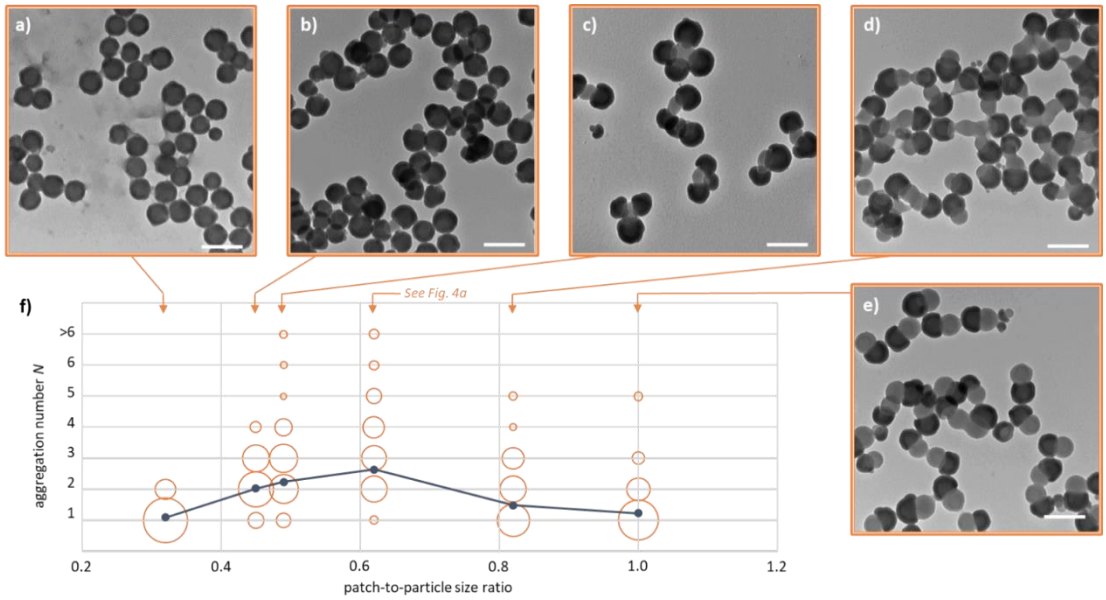

Fig. 5 a) to e) Representative TEM images of the cluster mixtures from the silica/PS dumbbell-shaped NPs as a function of the patch-to-particle size ratio corresponding to Batches #1 to #6 (scale bars: 200 nm); f) distribution of the NPs within the clusters of aggregation number *N* as determined by statistical analysis of the TEM images (the surface of the circles is proportional to the fraction of NPs assembled within clusters of similar aggregation number). The blue curve shows the evolution of the average aggregation number $\overline{N}$. Assembly experiments were performed in an ethanol/DMF mixture with a DMF fraction of 30 vol. % at a concentration of 5.3 × 10^{14} part/L at 20°C for 20 h with a final centrifugation stage (12,000 g for 10 min).

As expected, we observed that the lower relative size of the patch, the lower the average aggregation number. When it was 0.32 (Batch #1), only a few bipods were obtained ($\overline{N}$ = 1.10). The exclusive bipod morphology results from the steric hindrance of the silica lobes with regard to the PS sticking point,

making the cluster unable to attach a third NP. The low prevalence of the bipods can be explained by the small patch size, which decreases their probability of collision, i.e. the first stage of the assembly process. As far as the patch-to-particle size ratio was increased, $\bar{N}$ increased and reached a value of 2.65 (Batch #3, i.e. patch-to-particle size ratio of 0.62).

The results for higher patch-to-particle size ratios turned out to be unexpected because they showed a dramatic decrease of $\bar{N}$ down to 1.24 for Batch #6, i.e. patch-to-particle size ratio of 1.00. Moreover, the shape of clusters was not well defined and it was quite tricky to provide solid statistics data, especially for Batch #5. Nevertheless, we observed that for Batch #6, the average diameter of the PS lobes of the unassembled dumbbells decreased from 110 to 105 nm. This value fell to 102 nm and 96 nm when the solvent-induced assembly experiment was repeated using the same NP dispersion once and twice, respectively (after recovery by centrifugation and redispersion in ethanol). This means that, for the larger size of the PS protrusion, the amount of DMF was enough to extract a fraction of the PS chains, but not enough to make them sticky. We also tried to find again a better “sticky regime” by increasing the DMF fraction up to 50 vol. % with Batch #6 (Fig. 6). But unexpectedly, the “solvent regime” appeared from 45 vol. % with the appearance of a significant fraction of silica half-shells.

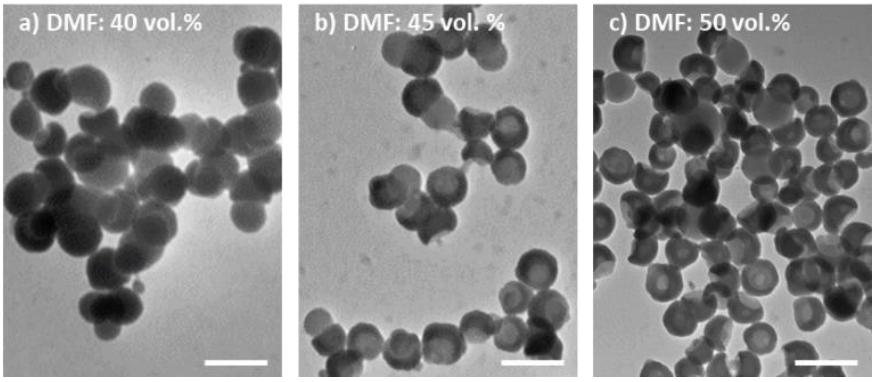

Fig. 6 Representative TEM images of the cluster mixtures of silica/PS dumbbell-shaped NPs from Batch #6 as a function of the DMF fraction in the ethanol/DMF mixture (scale bars: 200 nm). Assembly experiments were performed at a concentration of 5.3×10^{14} part/L at 20°C for 20 h with a final centrifugation stage (12,000 g for 10 min).

It can be concluded that quite unexpectedly the stickiness of the patch varies with the patch-to-particle size ratio, *i.e.* with the size of the PS lobe. We envisioned two assumptions to explain this phenomenon: (i) the PS chains in the smallest patches would make the latter more sticky, for instance, more easily swollen if they are particularly short and therefore less physically entangled, or (ii) the PS chains in the smallest patches would be more efficient for ensuring

the mechanical stability of the clusters and thereby making the assembly more irreversible.

Therefore, to go further in the interpretation, we measured by size-exclusion chromatography the molar mass distribution of the PS chains after extraction, *i.e.* the just-entangled macromolecules. This was performed in pure THF at RT for 2 h. After removal of the silica residue by centrifugation (12,000 g, 10 min), the samples were filtered and analysed by size exclusion chromatography in DMF. We observed that the molar mass distribution was made of three different macromolecular populations whatever the batch (See Supplementary material, Fig. S7):

i) the population with the highest molar mass ($M_{peak} \approx 2{,}000{,}000$ g/mol) corresponds to the MMS-crosslinked PS macromolecules that had never been covalently bonded to the silica shell;

ii) the 2nd population ($M_{peak} \approx 450{,}000$ g/mol) matches with the PS macromolecules of the initial seeds, because this quite large value is consistent with an emulsion polymerisation process using a water-soluble initiator;

iii) the 3rd population ($M_{peak} \approx 200{,}000$ g/mol) results from the polymerisation of the swollen styrene at the time of the symmetry breaking stage. This molar mass is lower because the process is closer to bulk polymerisation since AIBN is an organophilic initiator. AIBN decomposed into several free radical simultaneously, generating the high probability of termination reactions and a moderate molar mass.

As expected, we also observed that the higher the patch-to-particle size ratio, *i.e.* the larger the PS lobe, the higher the prevalence of this 3rd population with shorter chains. This result supports more readily the 2nd assumption: the largest PS lobes would be less efficient to maintain the cluster after coalescence because they would be softer than the smallest ones and the assembly would be more reversible, making $\bar{N}$ smaller. This could explain why with Batch #6 on Fig. 6b-c we observe the coexistence of apparently-intact silica/PS dumbbell-shaped NPs and silica half-shells. They could result indeed simply from a dissymmetric dislocation of clusters.

Cluster sorting by morphology

To further increase batch purity regarding cluster morphology, we verified that it is possible to purify the as-obtained batches by centrifugation (8,000 g; 20 min) in a linear gradient of sucrose (5-20 wt./vol.%) in water. In this way, purer batches were collected containing monopods (85%), bipods (52%), tripods

(48%) or tetrapods (53%) as shown in Fig.7. Batches with a higher purity would be readily achieved after the repetition and/or optimization of such a sorting process.

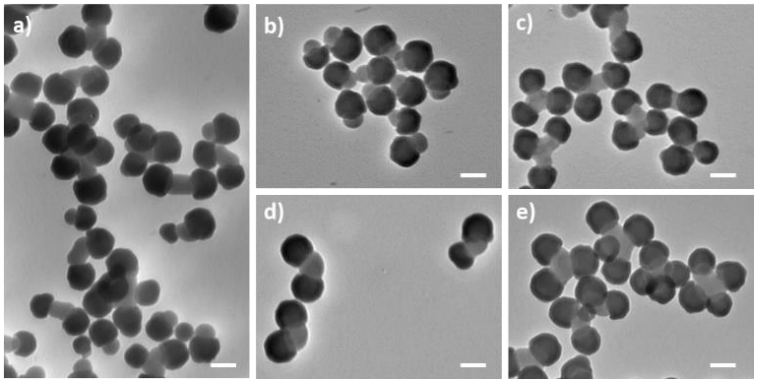

Fig. 7 Representative TEM images of a) the cluster mixture from silica/PS dumbbell-shaped NPs (Batch #3) as obtained after solvent-induced assembly and b-e) after sampling in the centrifugation tube in different bands (scale bars: 100 nm). Assembly experiments were performed in an ethanol/DMF mixture with DMF fraction of 30 vol. % at a concentration of 5.3 × 10^{14} part/L at 20°C for 20 h with a final centrifugation stage (12,000 g for 10 min). Sorting by centrifugation experiment was performed once at 8,000 g for 20 min in a sucrose gradient (5-20 wt./vol.%) in water.

Extending the strategy to gold-coated clusters

We extended the synthetic pathway to more complex building blocks, *i.e.* asymmetric dumbbells (Batch #3) whose silica lobe was previously decorated with gold seeds. The silica surface was first aminated by condensing aminopropyltriethoxysilane on the surface at RT in ethanol. The gold decoration stage used gold seeds (average size of 1-3 nm) stabilised with tetrakis(hydroxymethyl)phosphonium chloride. After assembly, clusters with *N* from 2 to 5 were observed (Fig. 8a-b). A subsequent gold regrowth stage using a gold plating solution and repeated three times appeared to be indeed site-specific because only silica lobes were covered by gold (Fig. 8c). However, the gold thickness was quite high and this induced that the silica lobes of the clusters were henceforth stuck together through the gold shell.

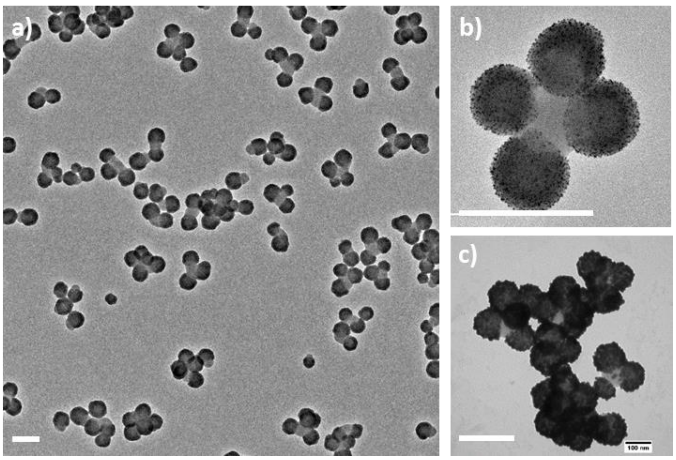

Fig. 8 Representative TEM images of (a) the cluster mixture from the asymmetric dumbbells previously gold-decorated on the silica lobe, (b) an enlarged view of a cluster with $N = 4$, and (c) the same cluster mixture after gold regrowth (scale bars: 200 nm). Assembly experiments after gold decoration of the asymmetric dumbbells (Batch #3) were performed in an ethanol/DMF mixture with DMF fraction of 30 vol. % at a concentration of 5.3×10^{14} part/L at 20°C for 20 min with a final centrifugation stage at 12,000 g for 10 min.

Alternatively, we first performed the gold regrowth of the gold seeds on the silica nodule to a final diameter of about 10 nm, *i.e.* decreasing the patch-to-particle size ratio from 0.62 to 0.52 (Fig. 9a). The assembly of these enlarged gold-decorated asymmetric dumbbells was successful at the expense of the adjustment of some experimental parameters because of the higher density of the building blocks: the centrifugation speed was reduced to 2,000 g and the DMF fraction was increased to 50 % (Fig. 9b-d)

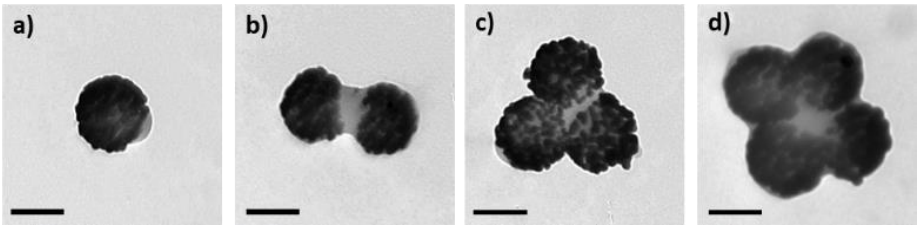

Fig. 9 Representative TEM images of (a) an asymmetric silica/PS dumbbell previously gold-decorated on the silica lobe, and clusters obtained after assembly of such dumbbells with (b) $N = 2$, (c) $N = 3$ and (d) $N = 4$ (scale bars: 100 nm). Assembly experiments were performed with the asymmetric dumbbells (Batch #3) in an ethanol/DMF mixture with DMF fraction of 50 vol. % at the concentration of 5.3×10^{14} part/L at 20°C for 20 min with a final centrifugation stage at 2,000 g for 10 min.

Conclusion

The dumbbells made of one silica lobe and one PS lobe, designed here as a sticky patch, were prepared successfully according to a protocol slightly adapted

from Guignard and Lattuada's protocol [22]**.** The ethanol/DMF mixture is a good medium to make the PS lobes sticky enough to coalesce with others at room temperature. The "sticky regime" corresponds to DMF fractions in the 30-50 vol. % range, which can be enlarged to 10-60 vol. % if the incubation process is completed with a centrifugation stage. The maximum aggregation numbers without and with centrifugation are 4 and more than 30, respectively. The role of the centrifugation remains poorly understood, and the effects of the NPs concentration and incubation time are quite moderate. The patch-to-particle size ratio was varied from 0.32 to 1.00 and its influence on the average aggregation number turned out to be partially unexpected. From 0.32 to 0.62, the larger the PS lobe, the higher the average aggregation number, in agreement with the widespread idea that the latter is mainly controlled by the steric hindrance of the non-sticky lobes. However, for the higher values of the patch-to-particle size ratio, the average aggregation number decreases, probably because the assembly is more reversible, *i.e.* the bonding within the clusters is less strong, owing to the larger fraction of shorter PS chains.

We showed that the proposed solvent-induced assembly route is efficient to prepare robust clusters in the 100-200 nm size range composed of a PS core and silica satellites. Compared to the previously-reported studies in the same size range [10], one of the main advantages of our clusters is their double chemical composition. Potential applications may concern the coating industry, where the performance of waterborne paints needs to be constantly improved [41].

The morphology of the as-obtained silica/PS clusters, *i.e.* colloidal molecules, is not as regular as the reverse morphology of the PS/silica multipods that we have investigated over the last decade [20,42]. Nevertheless, they could be optimised via the following strategy. As the cluster is built around a soft PS nodule, the conditions of its solidification determine the final geometry. For obtaining regular clusters, a slow solidification process combined with efficient repulsive forces between the silica satellites should be managed. This could be achieved by shifting slowly from the "sticky regime" to the "non-solvent regime" and by engineering the surface of the silica lobe to generate steric, electrostatic or electrosteric repulsion forces.

Lastly, we demonstrated that the solvent-induced self-assembly strategy could be extended to gold-coated clusters after slight optimisation of the experimental conditions. This opens avenues to new plasmonic building blocks with many potential applications in optics [43].

Conflicts of interest

There are no conflicts to declare.

Acknowledgments

This work was supported by the Agence Nationale de la Recherche (ENLARgER project, ANR-15-CE09-0010), the LabEx AMADEus (ANR-10-LABX-42) and IdEx Bordeaux (ANR-10-IDEX-03-02), that is, the Investissements d'Avenir programme of the French government managed by the Agence Nationale de la Recherche. Weiya Li was supported by a grant from the China Scholarship Council. Some of the TEM experiments were performed at the Plateforme de Caractérisation des Matériaux (UMS 3626, Pessac, France). The authors acknowledge gratefully Sylvain Bourasseau and Amélie Vax Weber for SEC experiments performed at the Laboratoire de Chimie des Polymères Organiques (UMR 5629, Pessac, France), Hervé Palis for density gradient centrifugation experiments, as well as Prof. Daniela J. Kraft (Leiden University, The Netherlands), Dr Corine Gérardin (CNRS-Montpellier, France) and Prof André Gröschel (University of Duisburg-Essen, Germany) for helpful discussion.

References

[1] M. Lattuada, T.A. Hatton, Synthesis, properties and applications of Janus nanoparticles, Nano Today. 6 (2011) 286–308. doi:10.1016/j.nantod.2011.04.008.

[2] A. Walther, A.H.E. Müller, Janus Particles: Synthesis, Self-Assembly, Physical Properties, and Applications, Chem. Rev. 113 (2013) 5194–5261. doi:10.1021/cr300089t.

[3] J. Zhang, B.A. Grzybowski, S. Granick, Janus Particle Synthesis, Assembly, and Application, Langmuir. 33 (2017) 6964–6977. doi:10.1021/acs.langmuir.7b01123.

[4] E. Bianchi, R. Blaak, C.N. Likos, Patchy colloids: state of the art and perspectives, Phys. Chem. Chem. Phys. 13 (2011) 6397. doi:10.1039/c0cp02296a.

[5] G.-R. Yi, D.J. Pine, S. Sacanna, Recent progress on patchy colloids and their self-assembly, J. Phys. Condens. Matter. 25 (2013) 193101. doi:10.1088/0953-8984/25/19/193101.

[6] S. Ravaine, E. Duguet, Synthesis and assembly of patchy particles: Recent progress and future prospects, Curr. Opin. Colloid Interface Sci. 30 (2017) 45–

53. doi:10.1016/j.cocis.2017.05.002.

[7] H. Hu, F. Ji, Y. Xu, J. Yu, Q. Liu, L. Chen, Q. Chen, P. Wen, Y. Lifshitz, Y. Wang, Q. Zhang, S.-T. Lee, Reversible and Precise Self-Assembly of Janus Metal-Organosilica Nanoparticles through a Linker-Free Approach, ACS Nano. 10 (2016) 7323–7330. doi:10.1021/acsnano.6b03396.

[8] N. Castro, D. Constantin, P. Davidson, B. Abécassis, Solution self-assembly of plasmonic Janus nanoparticles, Soft Matter. 12 (2016) 9666–9673. doi:10.1039/C6SM01632D.

[9] F. Liu, S. Goyal, M. Forrester, T. Ma, K. Miller, Y. Mansoorieh, J. Henjum, L. Zhou, E. Cochran, S. Jiang, Self-assembly of Janus Dumbbell Nanocrystals and Their Enhanced Surface Plasmon Resonance, Nano Lett. 19 (2019) 1587–1594. doi:10.1021/acs.nanolett.8b04464.

[10] D.J. Kraft, W.S. Vlug, C.M. van Kats, A. van Blaaderen, A. Imhof, W.K. Kegel, Self-Assembly of Colloids with Liquid Protrusions, J. Am. Chem. Soc. 131 (2009) 1182–1186. doi:10.1021/ja8079803.

[11] H. Liang, A. Cacciuto, E. Luijter, S. Granick, Clusters of charged janus spheres, Nano Lett. 6 (2006) 2510–2514. doi:10.1021/nl061857i.

[12] L. Hong, A. Cacciuto, E. Luijten, S. Granick, Clusters of amphiphilic colloidal spheres, Langmuir. 24 (2008) 621–625. doi:10.1021/la7030818.

[13] Q. Chen, J.K. Whitmer, S. Jiang, S.C. Bae, E. Luijten, S. Granick, Supracolloidal Reaction Kinetics of Janus Spheres, Science (80-.). 331 (2011) 199–202. doi:10.1126/science.1197451.

[14] D.J. Kraft, R. Ni, F. Smallenburg, M. Hermes, K. Yoon, D.A. Weitz, A. van Blaaderen, J. Groenewold, M. Dijkstra, W.K. Kegel, Surface roughness directed self-assembly of patchy particles into colloidal micelles, Proc. Natl. Acad. Sci. 109 (2012) 10787–10792. doi:10.1073/pnas.1116820109.

[15] B. Bharti, D. Rutkowski, K. Han, A.U. Kumar, C.K. Hall, O.D. Velev, Capillary Bridging as a Tool for Assembling Discrete Clusters of Patchy Particles, J. Am. Chem. Soc. 138 (2016) 14948–14953. doi:10.1021/jacs.6b08017.

[16] T.S. Skelhon, Y. Chen, S.A.F. Bon, Hierarchical self-assembly of ‘hard–soft’ Janus particles into colloidal molecules and larger supracolloidal structures, Soft Matter. 10 (2014) 7730–7735. doi:10.1039/C4SM01708K.

[17] A. Tsyrenova, K. Miller, J. Yan, E. Olson, S.M. Anthony, S. Jiang, Surfactant-Mediated Assembly of Amphiphilic Janus Spheres, Langmuir. 35 (2019) 6106–6111. doi:10.1021/acs.langmuir.9b00500.

[18] X.-H. Ge, Y.-H. Geng, J. Chen, J.-H. Xu, Smart Amphiphilic Janus Microparticles: One-Step Synthesis and Self-Assembly, ChemPhysChem. 19

(2018) 2009–2013. doi:10.1002/cphc.201700838.

[19] D.J. Kraft, J. Groenewold, W.K. Kegel, Colloidal molecules with well-controlled bond angles, Soft Matter. 5 (2009) 3823. doi:10.1039/b910593j.

[20] A. Perro, E. Duguet, O. Lambert, J.-C. Taveau, E. Bourgeat-Lami, S. Ravaine, A Chemical Synthetic Route towards “Colloidal Molecules,” Angew. Chemie Int. Ed. 48 (2009) 361–365. doi:10.1002/anie.200802562.

[21] C. Hubert, C. Chomette, A. Désert, M. Sun, M. Treguer-Delapierre, S. Mornet, A. Perro, E. Duguet, S. Ravaine, Synthesis of multivalent silica nanoparticles combining both enthalpic and entropic patchiness, Faraday Discuss. 181 (2015) 139–146. doi:10.1039/C4FD00241E.

[22] F. Guignard, M. Lattuada, Template-assisted synthesis of Janus silica nanobowls, Langmuir. 31 (2015) 4635–4643. doi:10.1021/acs.langmuir.5b00727.

[23] W. Stöber, A. Fink, E. Bohn, Controlled growth of monodisperse silica spheres in the micron size range, J. Colloid Interface Sci. 26 (1968) 62–69. doi:10.1016/0021-9797(68)90272-5.

[24] S. Zhang, W. Ni, X. Kou, M.H. Yeung, L. Sun, J. Wang, C. Yan, Formation of Gold and Silver Nanoparticle Arrays and Thin Shells on Mesostructured Silica Nanofibers, Adv. Funct. Mater. 17 (2007) 3258–3266. doi:10.1002/adfm.200700366.

[25] C. Chomette, M. Tréguer-Delapierre, N.B. Schade, V.N. Manoharan, O. Lambert, J.-C. Taveau, S. Ravaine, E. Duguet, Colloidal Alchemy: Conversion of Polystyrene Nanoclusters into Gold, ChemNanoMat. 3 (2017) 160–163. doi:10.1002/cnma.201600315.

[26] D.G. Duff, A. Baiker, P.P. Edwards, A new hydrosol of gold clusters. 1. Formation and particle size variation, Langmuir. 9 (1993) 2301–2309. doi:10.1021/la00033a010.

[27] E. Duguet, A. Désert, A. Perro, S. Ravaine, Design and elaboration of colloidal molecules: an overview, Chem. Soc. Rev. 40 (2011) 941. doi:10.1039/c0cs00048e.

[28] Y. Li, S. Chen, S. Demirci, S. Qin, Z. Xu, E. Olson, F. Liu, D. Palm, X. Yong, S. Jiang, Morphology evolution of Janus dumbbell nanoparticles in seeded emulsion polymerization, J. Colloid Interface Sci. 543 (2019) 34–42. doi:10.1016/j.jcis.2019.01.109.

[29] W.K. Kegel, D. Breed, M. Elsesser, D.J. Pine, Formation of anisotropic polymer colloids by disparate relaxation times, Langmuir. 22 (2006) 7135–7136. doi:10.1021/la061792z.

[30] J. Kim, R.J. Larsen, D.A. Weitz, Synthesis of Nonspherical Colloidal Particles with Anisotropic Properties, J. Am. Chem. Soc. 128 (2006) 14374–14377. doi:10.1021/ja065032m.

[31] E.B. Mock, H. De Bruyn, B.S. Hawkett, R.G. Gilbert, C.F. Zukoski, Synthesis of anisotropic nanoparticles by seeded emulsion polymerization, Langmuir. 22 (2006) 4037–4043. doi:10.1021/la060003a.

[32] J.-G. Park, J.D. Forster, E.R. Dufresne, High-Yield Synthesis of Monodisperse Dumbbell-Shaped Polymer Nanoparticles, J. Am. Chem. Soc. 132 (2010) 5960–5961. doi:10.1021/ja101760q.

[33] F. Sciortino, A. Giacometti, G. Pastore, Phase Diagram of Janus Particles, Phys. Rev. Lett. 103 (2009) 237801. doi:10.1103/PhysRevLett.103.237801.

[34] F. Sciortino, A. Giacometti, G. Pastore, A numerical study of one-patch colloidal particles: from square-well to Janus, Phys. Chem. Chem. Phys. 12 (2010) 11869. doi:10.1039/c0cp00504e.

[35] G. Munao, Z. Preisler, T. Vissers, F. Smallenburg, F. Sciortino, G. Munaò, Z. Preisler, T. Vissers, F. Smallenburg, F. Sciortino, Cluster formation in one-patch colloids: low coverage results, Soft Matter. 9 (2013) 2652–2661. doi:10.1039/c2sm27490f.

[36] Z. Preisler, T. Vissers, F. Smallenburg, G. Munaò, F. Sciortino, Phase Diagram of One-Patch Colloids Forming Tubes and Lamellae, J. Phys. Chem. B. 117 (2013) 9540–9547. doi:10.1021/jp404053t.

[37] T. Vissers, F. Smallenburg, G. Munaò, Z. Preisler, F. Sciortino, Cooperative polymerization of one-patch colloids, J. Chem. Phys. 140 (2014) 144902. doi:10.1063/1.4869834.

[38] G. Avvisati, T. Vissers, M. Dijkstra, Self-assembly of patchy colloidal dumbbells, J. Chem. Phys. 142 (2015) 084905. doi:10.1063/1.4913369.

[39] J.R. Bordin, L.B. Krott, Confinement effects on the properties of Janus dimers, Phys. Chem. Chem. Phys. 18 (2016) 28740–28746. doi:10.1039/C6CP05821C.

[40] C. Kang, A. Honciuc, Influence of Geometries on the Assembly of Snowman-Shaped Janus Nanoparticles, ACS Nano. 12 (2018) 3741–3750. doi:10.1021/acsnano.8b00960.

[41] S. Jiang, A. Van Dyk, A. Maurice, J. Bohling, D. Fasano, S. Brownell, Design colloidal particle morphology and self-assembly for coating applications, Chem. Soc. Rev. 46 (2017) 3792–3807. doi:10.1039/C6CS00807K.

[42] A. Désert, J. Morele, J.-C. Taveau, O. Lambert, M. Lansalot, E. Bourgeat-Lami, A. Thill, O. Spalla, L. Belloni, S. Ravaine, E. Duguet, Multipod-like

silica/polystyrene clusters, Nanoscale. 8 (2016) 5454–5469. doi:10.1039/C5NR07613G.

[43] V. Many, R. Dézert, E. Duguet, A. Baron, V. Jangid, V. Ponsinet, S. Ravaine, P. Richetti, P. Barois, M. Tréguer-Delapierre, High optical magnetism of dodecahedral plasmonic meta-atoms, Nanophotonics. 8 (2019) 549–558. doi:10.1515/nanoph-2018-0175.